

Lecture Notes in Mathematics

36

Edited by A. Dold and B. Eckmann

771

Approximation Methods for Navier-Stokes Problems

Proceedings of the Symposium Held by the
International Union of Theoretical and
Applied Mechanics (IUTAM)
at the University of Paderborn, Germany,
September 9 – 15, 1979

Edited by R. Rautmann



Springer-Verlag
Berlin Heidelberg New York 1980

EQUATIONS NEAR SHARP CORNERS

H.K. Moffatt

School of Mathematics

University of Bristol

Bristol BS8 2XL, U.K.

When the boundary of a fluid domain has any sharp corners, an understanding of the asymptotic structure of the flow near the corners is invariably helpful as a preliminary to determining the overall flow structure, and as a means of checking subsequent numerical calculations. The simplest example is that of Poiseuille flow along a sharp corner; a less simple example is the low Reynolds number flow between two hinged plates in relative angular motion. These problems are discussed here in §§1 and 2 (full details are given in Moffatt & Duffy 1979) and it is shown that the local similarity solution is not invariably asymptotically valid near the corner, but that it may (for certain ranges of corner angle) be dominated by 'eigenfunction' contributions which are sensitive to conditions remote from the corner. For critical angles, a transitional behaviour occurs.

In §§3-5, further examples are discussed of problems for which, despite the existence of a local similarity solution, the flow may (again for certain angle ranges) be dominated by eigenfunction contributions which may imply the presence of an infinite sequence of eddies in the corner (Moffatt 1964). These examples include the curved duct problem of Collins & Dennis (1976), the free convection problems of Liu & Joseph (1977), and the secondary flow problem in a cone-and-plate viscometer (Hynes 1978).

1. Poiseuille flow near a sharp corner

The following simple problem exemplifies a conflict between 'forced' solutions of similarity form and 'free' solutions of eigenfunction form which arises in the more complicated problems treated in subsequent sections. Consider steady pressure-driven flow along a straight duct whose cross-section \mathcal{D}_α is the sector of a circle illustrated in figure 1a.

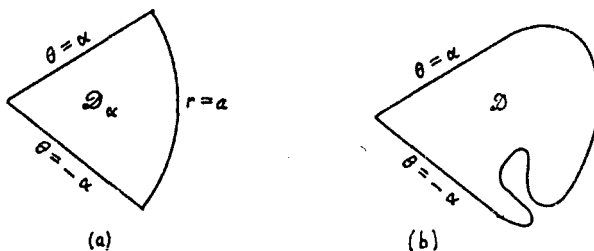


Figure 1. Cross-section of ducts; when $2\alpha < \pi/2$, the flow near 0 has the similarity form (1.2a); when $2\alpha > \pi/2$, it has the form (1.5) where A_0 depends on conditions far from the corner.

Taking polar coordinates (r, θ) , with origin at the corner, and axis $\theta = 0$ along the bisector of the angle, the velocity $w(r, \theta)$ satisfies

$$\nabla^2 w = -G/\mu \quad \text{in } \mathcal{D}_\alpha, \quad (1.1a)$$

$$w(r, \pm\alpha) = 0, \quad w(a, \theta) = 0, \quad (1.1b, c)$$

where G is the pressure gradient, μ the fluid viscosity, and 2α the angle of the corner. The (unique) solution to this problem is easily obtained in the form

$w = w_1 + w_2$, where

$$w_1 = \frac{Gr^2}{4\mu} \left(\frac{\cos 2\theta}{\cos 2\alpha} - 1 \right), \quad w_2 = \sum_{n=0}^{\infty} A_n r^{\lambda_n} \cos \lambda_n \theta, \quad (1.2a, b)$$

with

$$\lambda_n = \frac{(2n+1)\pi}{2\alpha}, \quad A_n = \frac{(-1)^{n+1} 2G a^{2-\lambda_n}}{\alpha \mu \lambda_n (\lambda_n^2 - 4)}. \quad (1.3a, b)$$

The contribution w_1 is a particular integral satisfying (1.1a, b) but not (1.1c); the contribution w_2 is a sum of eigenfunctions of the associated homogeneous problem

$$\nabla^2 w_2 = 0 \quad \text{in } \mathcal{D}_\alpha, \quad w_2(r, \pm\alpha) = 0, \quad (1.4)$$

with coefficients chosen so that $w = w_1 + w_2$ satisfies $w(a, \theta) = 0$ also.

Near the corner, the asymptotic form of w depends on the angle 2α . If $2\alpha < \pi/2$ (so that $\lambda_0 > 2$), then $w \sim w_1$, as $r \rightarrow 0$, i.e. the solution has a similarity form which does not depend on the radius a of the sector. This behaviour is insensitive to the 'remote geometry' of the cross-section, and we must evidently expect the same asymptotic behaviour if the remote boundary is distorted in any manner as in figure 1b.

If $2\alpha > \pi/2$ however, then $\lambda_0 < 2$, and so the leading term of the series for w_2 dominates as $r \rightarrow 0$, i.e.

$$w \sim A_0 r^{\pi/2\alpha} \cos(\pi\theta/2\alpha). \quad (1.5)$$

Here, A_0 does depend on the radius a (eqn. 1.3b), so that the solution cannot be regarded as locally determinate; indeed, although an asymptotic behaviour of the form (1.5) may be expected for the general geometry of figure 1b, the coefficient A_0 will in general depend on the shape of the portion of the boundary that is remote from the corner.

When $2\alpha = \pi/2$, the behaviour is evidently transitional. Putting $2\alpha = \pi/2 + \epsilon$ and letting $\epsilon \rightarrow 0$, we find

$$w \sim -\frac{Gr^2}{\pi\mu} \left[\frac{\pi}{4} + \left(\log \frac{r}{a} \right) \cos 2\theta - \theta \sin 2\theta \right]. \quad (1.6)$$

The singularity in w_1 when $2\alpha = \pi/2$ is compensated by an equal and opposite singularity in the first term of the series for w_2 . There is a similar cancellation with the second term when $2\alpha = 3\pi/2$.

2. The hinged plate and Jeffery-Hamel paradoxes

The apparent breakdown of a corner similarity solution at a critical value of the corner angle can occur in other circumstances, when the means of resolution may not be so obvious. Consider the problem depicted in figure 2a: fluid is contained in the angle between the two hinged plates which are rotated towards each other with angular velocities $\pm\omega$.

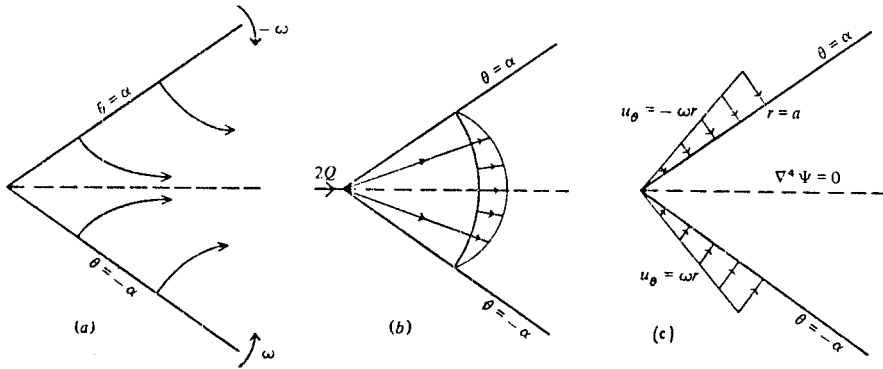


Figure 2. (a) The hinged plate problem; (b) the Jeffery-Hamel problem; (c) a hybrid problem which reduces to the hinged plate problem when $a \rightarrow \infty$ and to the Jeffery-Hamel problem when $a \rightarrow 0$, $\omega \rightarrow \infty$ with ωa^2 fixed.

Near the corner, inertia forces are negligible, and the stream function $\psi(r, \theta)$ satisfies the biharmonic equation $\nabla^4 \psi = 0$. The relevant similarity solution (Moffatt 1964) is

$$\gamma_1 = \frac{1}{2} \omega r^2 f(\theta), \quad f(\theta) = \frac{\sin 2\theta - 2\theta \cos 2\alpha}{\sin 2\alpha - 2\alpha \cos 2\alpha}, \quad (2.1a, b)$$

which is singular when $\tan 2\alpha = 2\alpha$, i.e. when $2\alpha \approx 257^\circ$ (more accurately 257.45°). A similar singularity occurs in the low Reynolds number version of the Jeffery-Hamel problem (figure 2b): if fluid is introduced at a volume rate $2Q$ per unit length of intersection, then the relevant solution is $\psi = Qf(\theta)$ where $f(\theta)$ is as defined by (2.1b) with the same singularity when $2\alpha \approx 257^\circ$.

The same type of paradox was identified and resolved, in an elasticity context, by Sternberg and Koiter (1958). We may resolve the difficulty here in a similar manner, by considering the problem sketched in figure 2c, in which (in effect) the source is distributed over a segment $0 < r < a$ of the two planes. This problem may be solved by means of the Mellin transform (for full details, see Moffatt and Duffy 1979). For $r < a$, the solution is given by a series

$$\psi = \omega a^2 \sum_{n=1}^{\infty} \left(\frac{r}{a}\right)^{p_n+2} f_n(\theta), \quad (2.2a)$$

where

$$f_n(\theta) = \frac{(p_n+2)^{-1} \cos p_n \alpha \sin(p_n+2)\theta - p_n^{-1} \cos(p_n+2)\alpha \sin p_n \theta}{\sin 2\alpha - 2\alpha \cos 2(p_n+1)\alpha}; \quad (2.2b)$$

here, the p_n are the (generally complex) roots of the equation

$$(p+1) \sin 2\alpha = \sin 2(p+1)\alpha, \quad (2.2c)$$

with $\text{Re } p_n > -1$, and ordered so that

$$-1 < p_1 \leq \text{Re } p_2 \leq \text{Re } p_3 \leq \dots \quad (2.2d)$$

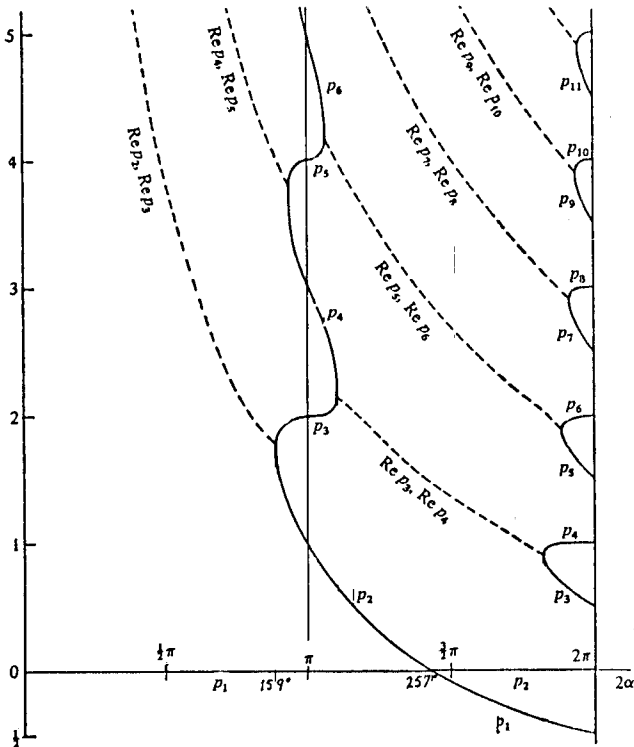


Figure 3. The real part of the roots p_n of equation (2.2c), as functions of the corner angle 2α . Where the n curves are solid, p_n is real; where they are dashed, p_n is complex, and only its real part is n shown. Note that $p_1 = 0$ for $2\alpha < 257^\circ$, $p_1 < 0$ for $2\alpha > 257^\circ$.

Figure 3 shows the rather interesting behaviour of $\text{Re } p_n$ ($n = 1, 2, \dots$) as functions of α ; note that p_1 is always real. For $r > a$, the is a proximity relation

$$\psi(r, \theta) = \left(\frac{r}{a}\right)^2 \psi\left(\frac{a}{r}, \theta\right), \quad (2.2e)$$

relating the solution to the expression (2.2a).

As $r/a \rightarrow 0$, (2.2a) generally gives the asymptotic behaviour

$$\psi \sim \omega a^2 \left(\frac{r}{a}\right)^{p_1+2} f_1(\theta). \quad (2.3)$$

For $2\alpha < 257^\circ$ (the root of $\tan 2\alpha = 2\alpha$), $p_1 = 0$ and (2.3) gives $\psi \sim \psi_1$ where ψ_1 is given by (2.1), i.e. the 'expected' similarity solution is indeed valid near the corner. Similarly, from (2.2e), for $r/a \rightarrow \infty$, $\psi \sim \omega a^2 f_1(\theta)$ which again has the expected similarity form. However, when $2\alpha > 257^\circ$, p_1 is negative (actually $-\frac{1}{2} < p_1 < 0$), and we do not recover the usual similarity solution; as in the simpler problem of §1, the solution for $r \rightarrow 0$ retains a dependence on the outer scale a , while for $r \rightarrow \infty$, the solution similarly retains a dependence on the inner scale a . Again, as we pass through the critical angle 257° (more accurately 257.45°), there is a transitional behaviour, the stream-function involving logarithmic terms.

3. Flow through curved ducts of triangular cross-section

In the examples discussed above, the simple similarity solution emerges as the particular integral of an inhomogeneous boundary-value problem, and its validity as an asymptotic solution breaks down whenever there is a solution of the associated homogeneous problem (i.e. a complementary function) which dominates over this particular integral. We now consider some further examples. Consider the problem of pressure-driven flow along a curved duct of triangular cross-section, as sketched in figure 4. It is supposed that the triangle is isosceles, the centre of curvature being on the line of symmetry of the section, and the angles of the triangle being β , β and 2α , with $\beta = \pi/2 - \alpha$. This configuration was studied numerically by Collins & Dennis (1976) in the particular case $2\alpha = \pi/2$, and with particular attention to the behaviour of the secondary flow in the cross-section and near the corners. When the curvature κ is small, the primary velocity component w in the duct is unaffected by the secondary flow, and is given by

$$\left. \begin{aligned} \nabla^2 w &= -G/\mu & \text{in } \mathcal{R}, \\ w &= 0 & \text{on } \partial\mathcal{R}. \end{aligned} \right\} \quad (3.1)$$

The stream function of the secondary flow is then determined by

$$\left. \begin{aligned} \nabla^4 \psi &= -2\kappa v^{-1} w \partial w / \partial y & \text{in } \mathcal{R} \\ \psi &= 0, \quad \partial\psi / \partial n = 0, & \text{on } \partial\mathcal{R} \end{aligned} \right\} \quad (3.2)$$

where the coordinate Oy is as indicated in figure 4, and v is the kinematic viscosity of the fluid. Consider first the behaviour near the corner A. Let (r, θ) be local polar coordinates; then $w = O(r^2)$ and $w \partial w / \partial y = O(r^3)$ near A, and, as pointed out by

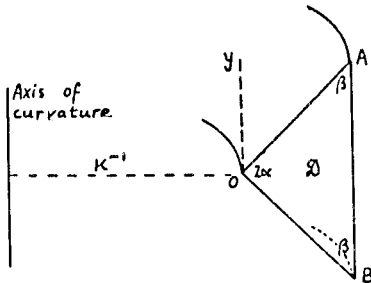


Figure 4. The curved duct configuration of Collins & Dennis (1976). When the flow is pressure-driven, eddies form at A and B if $\beta > 40.4^\circ$, and at O if $71.9^\circ < 2\alpha < 159.1^\circ$. When the flow is driven by rotation of the boundary AB about the axis of curvature (54), eddies do not form at A and B, but they do form at O if $35.0^\circ < 2\alpha < 159.1^\circ$.

Collins & Dennis, the particular integral of (3.2), ψ_1 say, is $O(r^7)$ near A. The dominant part of the complementary function has the form $r^\lambda f(\theta)$, where λ is complex. Near A, the flow certainly includes an ingredient whose r -component of velocity is antisymmetric about the corner bisector (we refer to this as an 'antisymmetric mode'), and the dependence of $\text{Re}\lambda$ on the corner angle (from tables given by Moffatt 1964) is as indicated in figure 5. If $\text{Re}\lambda < 7$, then the flow near A (and likewise of course near B) is characterised by an infinite sequence of corner eddies. From figure 5, this is the case for $\beta > 40.4^\circ$ (and in particular for the value $\beta = 45^\circ$ chosen by Collins & Dennis). If $\beta < 40.4^\circ$, then corner eddies will not form near A.

Consider now the situation near O. If $2\alpha < \pi/2$, then $w = O(r^2)$ where r is now distance from O, and again $\psi_1 = O(r^7)$. The secondary flow is symmetric about the bisector of the angle at O, and only symmetric eigenfunctions of the homogeneous problem are relevant. Again from figure 5, we find that, for the dominant symmetric mode, $\text{Re}\lambda < 7$ if $2\alpha > 71.9^\circ$. Hence corner eddies do not form at O if $2\alpha < 71.9^\circ$.

If $2\alpha > \pi/2$, then $w = O(r^{\pi/2\alpha})$ and so $\psi_1 = O(r^{\pi/\alpha + 3})$. It is easily ascertained that $\text{Re}\lambda < \pi/\alpha + 3$ for $\pi/2 < 2\alpha < \pi$, so that the complementary function dominates throughout this range; however λ is real for $2\alpha > 159.1^\circ$, and so corner eddies form at O only if $71.9^\circ < 2\alpha < 159.1^\circ$.

Ducts of other polygonal cross-sections could clearly be treated similarly.

4. Secondary eddies in circular Couette flow

Suppose now that the flow in the curved duct of figure 4 is generated not by a

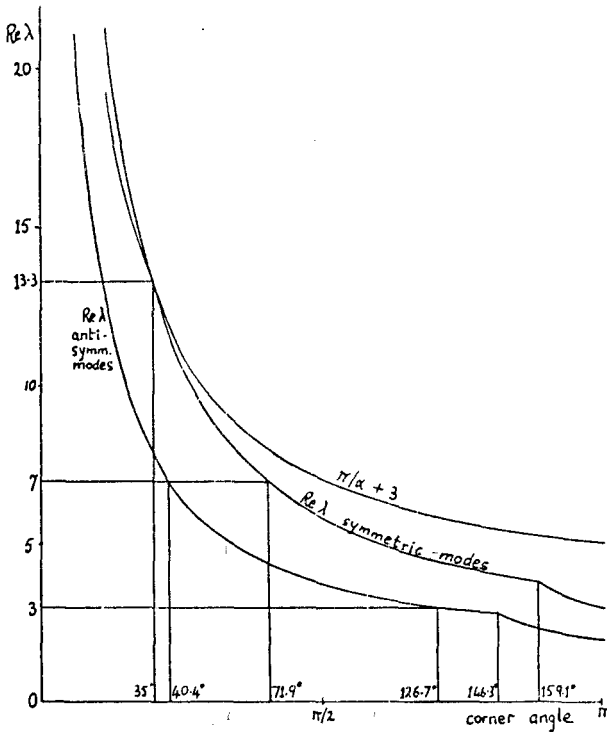


Figure 5. Variation of the real part of the exponent λ for symmetric and antisymmetric corner modes; note the jump in gradient at the critical angles (146.3° and 159.1°) where $\text{Im}\lambda = 0$ and corner eddies disappear.

pressure gradient, but by rotation of the cylindrical boundary AB about its axis of curvature, i.e. $w = w_0$ say on AB, while $w = 0$ on OA and OB. The primary flow is then of the Couette class, and $w = O(1)$ as $r \rightarrow 0$ (near A). Hence $w\partial w/\partial y = O(r^{-1})$ and so the particular integral of (3.2), ψ_1 , is $O(r^3)$ near A. The relevant exponent λ in the complementary function satisfies $\text{Re}\lambda > 3$ for all $\beta < \pi/2$, and so eddies do not form at A in this situation.

Near O, since there is no pressure gradient, we have $w = O(r^{\pi/2\alpha})$ and $\psi_1 = O(r^{\pi/\alpha+3})$, and eddies form if λ is complex and $\text{Re}\lambda < \pi/\alpha + 3$; from figure 5, this condition is satisfied when $2\alpha > 35.0^\circ$, (but it will be noticed that we have here a situation where the particular integral and complementary function have nearly the same exponent over a wide range of corner angles). The range of angles over which

corner eddies will form is

$$35.0^\circ < 2\alpha < 159.1^\circ. \quad (4.1)$$

There is a related behaviour in a situation studied by Hynes (1978), viz. the flow in the space between two cones (angles α , β with $\alpha < \beta$) with common vertex and axis of symmetry, when one of the cones is rotated about the axis of symmetry, the other being fixed (figure 6a). If $\beta = \pi/2$ and the inner cone is rotated, we have

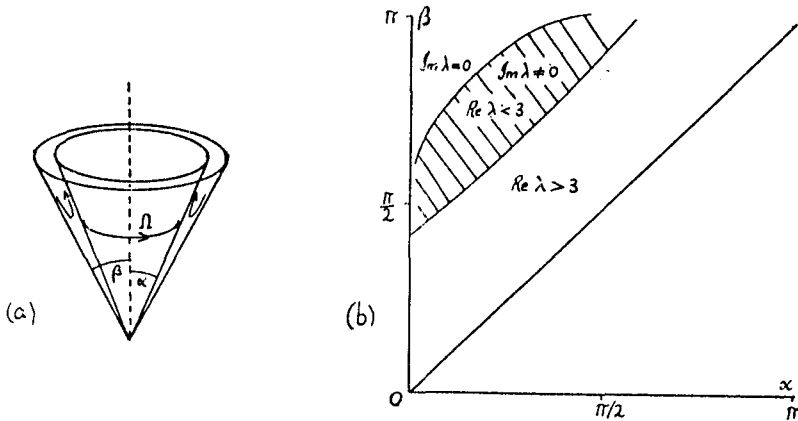


Figure 6. (a) Secondary flow between two cones, the inner one rotating. (b) The shaded area corresponds to values of α and β for which an infinite sequence of toroidal vortices occurs near the vertex.

here the familiar configuration of the cone-and-plate viscometer. The appearance of eddies (or rather toroidal vortices) in the secondary flow is often interpreted as a manifestation of non-Newtonian behaviour. However, Hynes has shown that eddies will occur even in a Newtonian fluid for a certain range of values of α and β . The primary flow component is azimuthal and has the form $w = rf(\theta)$. The corresponding forced secondary flow is $O(r^3)$ as $r \rightarrow 0$. The Stokes stream-function ψ consists again of two parts, the forced ingredient $\psi_1 = O(r^5)$, and the complementary function ψ_2 which satisfies

$$\left. \begin{aligned} D^4 \psi_2 &= 0 & (\alpha < \theta < \beta) \\ \partial \psi_2 / \partial \theta = \psi_2 &= 0 & (\theta = \alpha, \theta = \beta) \end{aligned} \right\} \quad (4.2)$$

where D^2 is the Stokes operator. This admits solutions of the form

$$\psi_2 = r^{\lambda+2} f_2(\theta), \quad (4.3)$$

and this dominates over ψ_1 near $r = 0$ if $\text{Re}\lambda < 3$. Toroidal vortices therefore occur near 0 if $\text{Re}\lambda < 3$ and $\text{Im}\lambda \neq 0$. Figure 6b (inferred from Hynes 1978) shows the region of the (α, β) plane in which these conditions are simultaneously satisfied. In the cone and plate viscometer situation ($\beta = \pi/2$), eddies will not form if $\sigma > 15^\circ$. If eddies do appear for $\alpha > 15^\circ$, then this must indeed be due to non-Newtonian effects (see, for example, Rivlin 1976).

5. Corner flows driven by heating

Finally, let us apply similar considerations to flows of the type studied by Liu & Joseph (1977), as depicted in figure 7. The applied temperature difference ΔT induces a temperature field $T(r, \theta)$ in the fluid, and the resulting buoyancy force

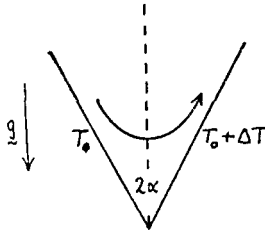


Figure 7. Corner flow driven by side-wall heating (Liu & Joseph 1977). Corner eddies occur if $126.7^\circ < 2\alpha < 146.3^\circ$.

drives the motion. Sufficiently near the corner, T satisfies $\nabla^2 T = 0$, and so $T \sim T_0 + \Delta T f(\theta)$ as $r \rightarrow 0$. Hence $\nabla T = O(r^{-1})$, and the resulting forced ingredient ψ_1 of the stream-function is $O(r^3)$. This is like the situation studied in §4, and we know that corner eddies will not occur if $2\alpha < \pi/2$. Liu & Joseph gave full details for the cases $2\alpha = 10^\circ, 60^\circ$ and found that the forced ingredient indeed dominated in these cases.

When $2\alpha > \pi/2$, the condition $\text{Re}\lambda < 3$ is satisfied if $2\alpha > 126.7^\circ$ (figure 5), and λ is real if $2\alpha < 146.3^\circ$; hence corner eddies may be expected to form for

$$126.7^\circ < 2\alpha < 146.3^\circ, \quad (5.1)$$

although again, the forced and free solutions are finely balanced in this range of angles ($\text{Re}\lambda \approx 2.8$ when $2\alpha = 146.3^\circ$)

Acknowledgements

The work described in §§1 and 2 was carried out in collaboration with Dr. B.R. Duffy and is supported by S.R.C. Research Grant No. GR/A/5593.4.

References

- Collins, W.M. & Dennis, S.C.R. 1976. Viscous eddies near a 90° and a 45° corner. Flow through a curved tube of triangular cross-section. *J.Fluid Mech.* 76, 417.
- Hynes, T. 1978. Slow viscous flow between cones. Ph.D. thesis, Cambridge University.
- Liu, C.H. & Joseph, D.D. 1977. Stokes flow in wedge-shaped trenches. *J.Fluid Mech.* 80, 443-463.
- Moffatt, H.K. 1964. Viscous and resistive eddies near a sharp corner. *J.Fluid Mech.* 18, 1-18.
- Moffatt, H.K. & Duffy, B.R. 1979. Local similarity solutions and their limitations. *J.Fluid Mech.* (to appear).
- Rivlin, R.S. 1977. Secondary flows in viscoelastic fluids. in *Theoretical and Applied Mechanics, Proc. 14th IUTAM Congress, Delft 1976*, Ed. W. Koiter, North Holland Publ.Co., 221-232.